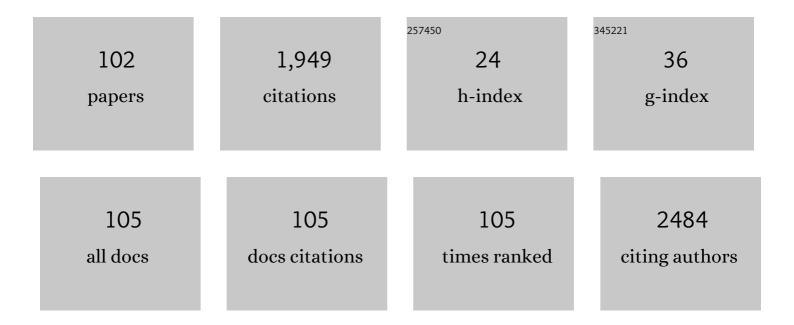
Zi-Sheng Chao

List of Publications by Year in descending order

Source: https://exaly.com/author-pdf/2035059/publications.pdf Version: 2024-02-01



#	Article	IF	CITATIONS
1	Pseudocapacitive Contribution in Amorphous FeVO ₄ Cathode for Lithiumâ€lon Batteries. ChemElectroChem, 2022, 9, .	3.4	2
2	Approaching theoretical specific capacity of iron-rich lithium iron silicate using graphene-incorporation and fluorine-doping. Journal of Materials Chemistry A, 2022, 10, 4006-4014.	10.3	10
3	New Type of SnSe/CoSe@C Anode for Lithium-Ion Batteries. Energy & Fuels, 2022, 36, 2260-2267.	5.1	13
4	A novel honeycomb-like WS2-x/CoS@C composite as anode for lithium ion batteries. Journal of Materials Science, 2022, 57, 5118-5129.	3.7	5
5	Metal-Porphyrin Frameworks Supported by Carbon Nanotubes: Efficient Polysulfide Electrocatalysts for Lithium-Sulfur Batteries. Chemical Engineering Journal, 2022, 437, 135150.	12.7	8
6	Synthesis of three-dimensional multifunctional Co3O4 nanostructures for electrochemical supercapacitors and H2 production. Journal of Materials Science: Materials in Electronics, 2022, 33, 10207-10225.	2.2	2
7	Synthesis of Cobalt Diselenide Nanoparticles for the Integrated All-Solid-State Supercapacitors. Energy & Fuels, 2022, 36, 5928-5936.	5.1	7
8	Stable WS ₂ /WO ₃ Composites as High-Performance Cathode for Rechargeable Aluminum-Ion Batteries. Energy & Fuels, 2022, 36, 7890-7897.	5.1	8
9	Oxygen Vacancy-Rich Mixed-Valence Cerium MOF: An Efficient Separator Coating to High-Performance Lithium–Sulfur Batteries. ACS Applied Materials & Interfaces, 2021, 13, 3899-3910.	8.0	65
10	Low-temperature preparation achieving 10.95%-efficiency of hole-free and carbon-based all-inorganic CsPbI3 perovskite solar cells. Journal of Alloys and Compounds, 2021, 862, 158454.	5.5	25
11	Study on the Ion Substitution Mechanism of CsPbIBr ₂ Films Prepared by a Drop-Coating Method. ACS Applied Energy Materials, 2021, 4, 4686-4694.	5.1	7
12	A Novel MoS ₂ -MXene Composite Cathode for Aluminum-Ion Batteries. Energy & Fuels, 2021, 35, 12666-12670.	5.1	33
13	Effect of Thin Film to Boost the Electrochemical Properties of LiMn _{1.5} Ni _{0.5} O ₄ . Energy & Fuels, 2021, 35, 15166-15171.	5.1	5
14	In situ-grown Co3O4 nanorods on carbon cloth for efficient electrocatalytic oxidation of urea. Journal of Nanostructure in Chemistry, 2021, 11, 735-749.	9.1	25
15	Hierarchical ZnO/MXene composites and their photocatalytic performances. Colloids and Surfaces A: Physicochemical and Engineering Aspects, 2021, 628, 127230.	4.7	36
16	All-inorganic, hole-transporting-layer-free, carbon-based CsPbIBr2 planar solar cells with ZnO as electron-transporting materials. Journal of Alloys and Compounds, 2020, 817, 152768.	5.5	22
17	Three dimensional Ni ₃ S ₂ nanorod arrays as multifunctional electrodes for electrochemical energy storage and conversion applications. Nanoscale Advances, 2020, 2, 478-488.	4.6	9
18	MCM-22 Zeolite-Induced Synthesis of Thin Sodalite Zeolite Membranes. Chemistry of Materials, 2020, 32, 333-340.	6.7	16

#	Article	IF	CITATIONS
19	Synthesis of superhydrophobic flower-like ZnO on nickel foam. CrystEngComm, 2020, 22, 205-212.	2.6	15
20	Effects of bubbles on the structure and performance of zeolite membranes. Journal of the European Ceramic Society, 2020, 40, 1709-1716.	5.7	5
21	Facile fabrication of \$\$hbox {CeO}_{2}\$\$ nanomaterials by hydrothermal methods and their photocatalytic and hydrophobic properties. Bulletin of Materials Science, 2020, 43, 1.	1.7	2
22	Postmetalation of a new porphyrin ligand-based metal–organic framework for catalytic oxidative carboxylation of olefins. Journal of Materials Science, 2020, 55, 16184-16196.	3.7	16
23	Celgard-supported LiX zeolite membrane as ion-permselective separator in lithium sulfur battery. Journal of Membrane Science, 2020, 611, 118386.	8.2	40
24	Introduction of an interface layer on hydroxyapatite whisker/poly(L-lactide) composite and its contribution for improved bioactivity and mechanical properties. Nanotechnology, 2020, 31, 235703.	2.6	1
25	Fundamental Study toward Improving the Performance of a High-Moisture Biomass-Fueled Redox Flow Fuel Cell. Industrial & Engineering Chemistry Research, 2020, 59, 4817-4828.	3.7	14
26	Perovskite Lithium Lanthanum Titanate-Modified Separator as Both Adsorbent and Converter of Soluble Polysulfides toward High-Performance Li-S Battery. ACS Sustainable Chemistry and Engineering, 2020, 8, 16477-16492.	6.7	20
27	A TiO ₂ /C catalyst having biomimetic channels and extremely low Pt loading for formaldehyde oxidation. RSC Advances, 2019, 9, 3965-3971.	3.6	9
28	UV-resistant hydrophobic CeO2 nanomaterial with photocatalytic depollution performance. Ceramics International, 2018, 44, 13439-13443.	4.8	17
29	Poly(l-lactide)/cyclodextrin/citrate networks modified hydroxyapatite and its role as filler in the promotion to the properties of poly(l-lactide) biomaterials. Polymer, 2018, 145, 1-10.	3.8	5
30	Effective ternary copper-cerium-cobalt catalysts synthesized via a modified pechini method for selective oxidation of ethylbenzene. Materials Chemistry and Physics, 2018, 214, 239-246.	4.0	23
31	Synthesis of a ZSM-5/NaA hybrid zeolite membrane using kaolin as a modification layer. New Journal of Chemistry, 2018, 42, 6664-6672.	2.8	7
32	Synthesis of NaA zeolite membrane by maintaining pressure difference between the two sides of the support. CrystEngComm, 2018, 20, 7195-7205.	2.6	9
33	Study on screening catalysts for the synthesis of acrolein diethyl acetal/ammonia toward pyridine and 3-picoline. AIP Conference Proceedings, 2018, , .	0.4	0
34	Enhanced sunlight-driven photocatalytic property of Mg-doped ZnO nanocomposites with three-dimensional graphene oxide/MoS ₂ nanosheet composites. RSC Advances, 2018, 8, 17399-17409.	3.6	22
35	High efficiency microwave-assisted synthesis of quinoline from acrolein diethyl acetal and aniline utilizing Ni/Beta catalyst. Catalysis Communications, 2018, 115, 21-25.	3.3	11
36	Synthesis of poly(<scp>l</scp> -lactide)/β-cyclodextrin/citrate network modified hydroxyapatite and its biomedical properties. New Journal of Chemistry, 2018, 42, 14729-14732.	2.8	11

#	Article	IF	CITATIONS
37	SPEEK Membrane of Ultrahigh Stability Enhanced by Functionalized Carbon Nanotubes for Vanadium Redox Flow Battery. Frontiers in Chemistry, 2018, 6, 286.	3.6	49
38	Low-temperature construction of MoS2 quantum dots/ZnO spheres and their photocatalytic activity under natural sunlight. Journal of Colloid and Interface Science, 2018, 530, 714-724.	9.4	32
39	UVâ€Resistant and Thermally Stable Superhydrophobic CeO ₂ Nanotubes with High Water Adhesion. Small, 2018, 14, e1801040.	10.0	32
40	WO ₃ Quantum Dots Decorated GO/Mgâ€doped ZnO Composites for Enhanced Photocatalytic Activity under Nature Sunlight. Applied Organometallic Chemistry, 2018, 32, e4449.	3.5	18
41	Efficient Biomass Fuel Cell Powered by Sugar with Photo―and Thermalâ€Catalysis by Solar Irradiation. ChemSusChem, 2018, 11, 2229-2238.	6.8	19
42	Facile Fabrication of ZnO Nanomaterials and Their Photocatalytic Activity Study. Science of Advanced Materials, 2018, 10, 1721-1728.	0.7	16
43	Patching NaA zeolite membrane by adding methylcellulose into the synthesis gel. Journal of Membrane Science, 2017, 530, 240-249.	8.2	16
44	High-efficiency catalytic performance over mesoporous Ni/beta zeolite for the synthesis of quinoline from glycerol and aniline. RSC Advances, 2017, 7, 9551-9561.	3.6	29
45	ZIF-67 derived Ag-Co 3 O 4 @N-doped carbon/carbon nanotubes composite and its application in Mg-air fuel cell. Electrochemistry Communications, 2017, 77, 5-9.	4.7	32
46	A novel approach to vapor-phase synthesis of 2- and 4-methylquinoline from lactic acid and aniline. Catalysis Communications, 2017, 98, 13-16.	3.3	5
47	Synthesis of quinolines from aniline and propanol over modified USY zeolite: catalytic performance and mechanism evaluated by in situ Fourier transform infrared spectroscopy. RSC Advances, 2017, 7, 24950-24962.	3.6	13
48	Synthesis of <scp>l</scp> -Lactide via Degradation of Various Telechelic Oligomeric Poly(<scp>l</scp> -lactic acid) Intermediates. Industrial & Engineering Chemistry Research, 2017, 56, 4867-4877.	3.7	15
49	Hydrogenation of 3-hydroxypropanal to 1,3-propanediol over a Cu–V/Ni/SiO ₂ catalyst. New Journal of Chemistry, 2017, 41, 8965-8976.	2.8	3
50	Hydrogenation of 3-hydroxypropanal into 1,3-propanediol over bimetallic Ru–Ni catalyst. RSC Advances, 2017, 7, 32027-32037.	3.6	16
51	Heterogeneous catalytic synthesis of quinoline compounds from aniline and C1–C4 alcohols over zeolite-based catalysts. RSC Advances, 2017, 7, 48275-48285.	3.6	15
52	The mild liquid-phase synthesis of 3-picoline from acrolein diethyl acetal and ammonia over heterogeneous catalysts. IOP Conference Series: Earth and Environmental Science, 2017, 94, 012031.	0.3	0
53	Super-hydrophobic Co3O4-loaded nickel foam with corrosion-resistant property prepared by combination of hydrothermal synthesis and PFAS modification. Surface and Coatings Technology, 2017, 309, 1111-1118.	4.8	16
54	High performance super-hydrophobic ZrO2-SiO2 porous ceramics coating with flower-like CeO2 micro/nano-structure. Surface and Coatings Technology, 2017, 325, 565-571.	4.8	16

#	Article	IF	CITATIONS
55	Dehydration of bio-ethanol to ethylene over iron exchanged HZSM-5. Chinese Journal of Catalysis, 2016, 37, 1941-1948.	14.0	22
56	α-MnO 2 Nanowires/Graphene Composites with High Electrocatalytic Activity for Mg-Air Fuel Cell. Electrochimica Acta, 2016, 219, 492-501.	5.2	44
57	Methylcellulose-assisted synthesis of a compact and thin NaA zeolite membrane. RSC Advances, 2016, 6, 71863-71866.	3.6	10
58	Green Synthesis of <i>N</i> , <i>N</i> ′-Dialkylureas from CO ₂ and Amines Using Metal Salts of Oxalates as Catalysts. Industrial & Engineering Chemistry Research, 2016, 55, 64-70.	3.7	24
59	Microwave-accelerated direct synthesis of 3-picoline from glycerol through a liquid phase reaction pathway. New Journal of Chemistry, 2016, 40, 8863-8871.	2.8	7
60	Deactivation and regeneration on the ZSM-5-based catalyst for the synthesis of pyridine and 3-picoline. Microporous and Mesoporous Materials, 2016, 235, 261-269.	4.4	15
61	Preparation of pyridine and 3-picoline from acrolein and ammonia with HF/MgZSM-5 catalyst. Catalysis Communications, 2016, 80, 10-14.	3.3	16
62	High efficiency hydrogen evolution from native biomass electrolysis. Energy and Environmental Science, 2016, 9, 467-472.	30.8	140
63	Towards a full understanding of the nature of Ni(<scp>ii</scp>) species and hydroxyl groups over highly siliceous HZSM-5 zeolite supported nickel catalysts prepared by a deposition–precipitation method. Dalton Transactions, 2016, 45, 2720-2739.	3.3	50
64	Mechanism of pyridine bases prepared from acrolein and ammonia by in situ infrared spectroscopy. Journal of Molecular Catalysis A, 2016, 411, 19-26.	4.8	17
65	Influence of Reaction Parameters on the Catalytic Performance of Alkaline-Treated Zeolites in the Novel Synthesis of Pyridine Bases from Glycerol and Ammonia. Industrial & Engineering Chemistry Research, 2016, 55, 893-911.	3.7	28
66	The synthesis of pyridine and 3-picoline from gas-phase acrolein diethyl acetal with ammonia over ZnO/HZSM-5. Chemical Engineering Journal, 2015, 273, 7-18.	12.7	28
67	Unsaturated aldehydes: a novel route for the synthesis of pyridine and 3-picoline. RSC Advances, 2015, 5, 54090-54101.	3.6	12
68	Dynamic Lithium Intercalation/Deintercalation in 18650 Lithium Ion Battery by Time-Resolved High Energy Synchrotron X-Ray Diffraction. Journal of the Electrochemical Society, 2015, 162, A2195-A2200.	2.9	17
69	A simple and convenient approach for preparing core–shell-like silica@nickel species nanoparticles: highly efficient and stable catalyst for the dehydrogenation of 1,2-cyclohexanediol to catechol. Dalton Transactions, 2015, 44, 1023-1038.	3.3	14
70	Synthesis of 3-picoline from acrolein and ammonia through a liquid-phase reaction pathway using SO42â^'/ZrO2-FeZSM-5 as catalyst. Chemical Engineering Journal, 2014, 253, 544-553.	12.7	26
71	Role of Na in the dehydro-aromatization of 1,2-cyclohexanediol to catechol over the Na/Ni/HZSM-5 catalyst. Applied Catalysis A: General, 2014, 470, 239-249.	4.3	11
72	Phosgene-free synthesis of hexamethylene-1,6-diisocyanate by the catalytic decomposition of dimethylhexane-1,6-dicarbamate over zinc-incorporated berlinite (ZnAlPO4). Journal of Hazardous Materials, 2014, 266, 167-173.	12.4	22

#	Article	IF	CITATIONS
73	Synthesis of High-Performanced Titanium Silicalite-1 Zeolite at Very Low Usage of Tetrapropyl Ammonium Hydroxide. Industrial & Engineering Chemistry Research, 2013, 52, 3762-3772.	3.7	33
74	Dynamic study of Li intercalation into graphite by in situ high energy synchrotron XRD. Electrochimica Acta, 2013, 92, 148-152.	5.2	89
75	Synthesis of mesoporous chromium phosphatesvia solid-state reaction at low temperature. New Journal of Chemistry, 2012, 36, 139-147.	2.8	10
76	Synthesis of mesoporous chromium aluminophosphate (CrAlPO) via solid state reaction at low temperature. Journal Wuhan University of Technology, Materials Science Edition, 2012, 27, 337-345.	1.0	2
77	Ethanol-assistant synthesis of TS-1 containing no extra-framework Ti species. Catalysis Today, 2010, 158, 510-514.	4.4	25
78	CH3COONa as an effective catalyst for methoxycarbonylation of 1,6-hexanediamine by dimethyl carbonate to dimethylhexane-1,6-dicarbamate. Green Chemistry, 2010, 12, 483.	9.0	40
79	Replication Route Synthesis of Mesoporous Titanium–Cobalt Oxides and Their Photocatalytic Activity in the Degradation of Methyl Orange. Catalysis Letters, 2009, 129, 26-38.	2.6	8
80	Synthesis of micro- and mesoporous ZSM-5 composites and their catalytic application in glycerol dehydration to acrolein. Studies in Surface Science and Catalysis, 2007, , 527-530.	1.5	25
81	A novel synthesis of manganese oxide nanotubes. Studies in Surface Science and Catalysis, 2007, 165, 313-316.	1.5	2
82	Synthesis and characterization of lanthanum oxide nanotubes using dendritic surfactant. Studies in Surface Science and Catalysis, 2007, 165, 339-342.	1.5	4
83	Catalysis over zinc-incorporated berlinite (ZnAlPO4) of the methoxycarbonylation of 1,6-hexanediamine with dimethyl carbonate to form dimethylhexane-1,6-dicarbamate. Chemistry Central Journal, 2007, 1, 27.	2.6	38
84	Preparation of NaA Zeolite Membrane with High Permeability by Using a Modified VPT Method. Chemistry Letters, 2006, 35, 1056-1057.	1.3	9
85	1-(3,5-Dichlorophenyl)-3-trifluoromethyl-1H-pyrazol-5-yl 2-chlorobenzoate. Acta Crystallographica Section E: Structure Reports Online, 2006, 62, o505-o507.	0.2	Ο
86	A redox-assisted supramolecular assembly of manganese oxide nanotube. Materials Research Bulletin, 2006, 41, 2035-2040.	5.2	8
87	Preparation and characterization of hexagonal mesoporous titanium–cobalt oxides. Materials Letters, 2006, 60, 2115-2118.	2.6	3
88	V–Mg–O Prepared via a Mesoporous Pathway: A Low-Temperature Catalyst for the Oxidative Dehydrogenation of Propane to Propene. Catalysis Letters, 2004, 94, 217-221.	2.6	23
89	Noncatalytic and catalytic conversion of ethane over Vî—,Mg oxide catalysts prepared via solid reaction or mesoporous precursors. Journal of Catalysis, 2004, 222, 17-31.	6.2	33
90	Specific Ion and pH Effects on Supramolecular Assembly of Mesostructured Vâ^'Mg Oxides. Langmuir, 2004, 20, 7517-7525.	3.5	4

#	Article	IF	CITATIONS
91	Title is missing!. Catalysis Letters, 2003, 88, 147-154.	2.6	12
92	Phase Behavior of Mesostructured V-Mg-O. Langmuir, 2003, 19, 4235-4245.	3.5	5
93	NaA Zeolite Membrane with High Performance Synthesized by Vapor Phase Transformation Method. Chinese Journal of Chemistry, 2003, 21, 1430-1432.	4.9	13
94	Nanosized NaY Zeolite Synthesized Rapidly by Microwave Induction. Wuli Huaxue Xuebao/ Acta Physico - Chimica Sinica, 2003, 19, 487-491.	4.9	9
95	Effect of the Nature of the Templating Surfactant on the Synthesis and Structure of Mesoporous Vâ^'Mgâ^'O. Langmuir, 2002, 18, 734-743.	3.5	24
96	Structural and Morphological Control of Mesostructures: Vanadium Based Nanofibers. Chemistry of Materials, 2002, 14, 4611-4618.	6.7	13
97	Control of Magnesium Containing Vanadium Mesoporous Materials. Langmuir, 2002, 18, 8535-8545.	3.5	9
98	Synthesis of Mesoporous Vâ^'Mgâ^'O Nanofibers. Nano Letters, 2001, 1, 739-742.	9.1	13
99	1H MAS NMR characterization of hydrogen over silica-supported rhodium catalyst. Science in China Series B: Chemistry, 2001, 44, 103-112.	0.8	4
100	Mechanistic study of partial oxidation of methane to synthesis gas over supported rhodium and ruthenium catalysts using in situ time-resolved FTIR spectroscopy. Catalysis Today, 2000, 63, 317-326.	4.4	68
101	In situ time-resolved FTIR investigation on the reaction mechanism of partial oxidation of methane to syngas over supported Rh and Ru catalysts. Science Bulletin, 2000, 45, 2236-2240.	1.7	3
102	Constituent selection and performance characterization of catalysts for oxidative coupling of methane and oxidative dehydrogenation of ethane. Catalysis Today, 1996, 30, 67-76.	4.4	41